NANOSYSTEMS:
PHYSICS, CHEMISTRY, MATHEMATICS

Original article

Novikova S.A., et al. *Nanosystems: Phys. Chem. Math.*, 2025, **16** (4), 521–527.
http://nanojournal.ifmo.ru
DOI 10.17586/2220-8054-2025-16-4-521-527

A surface modification strategy for synthesizing highly water-stable $CsPbBr_3$ perovskite quantum dots

Sagila A. Novikova[1,a], Elena D. Gribova[1,b], Ksenia S. Kasimtseva[1,c],
Evgeniy A. Sidorov[1,d], I. N. Fadeikina[2], A. N. Nechaev[2]

[1]Dubna State University, Dubna, Moscow oblast, 141980, Russia
[2]Joint Institute for Nuclear Research, Dubna, Moscow oblast, 141980 Russia

[a]sagila@uni-dubna.ru, [b]elena_g67@mail.ru, [c]kasimtseva20@yandex.ru, [d]zhenya.sidorov1@gmail.com

Corresponding author: S. A. Novikova, sagila@uni-dubna.ru

PACS 61.46.Df, 73.21.La, 61.46.+w

ABSTRACT Hydrophobic $CsPbBr_3$ perovskite quantum dots (PQDs) were synthesized via a ligand-assisted re precipitation method with various antisolvents. A study was conducted to assess antisolvents influence on the properties of the synthesized PQDs. To enhance the stability of PQDs in polar media and possess surface functional groups for further conjugation with biomolecules, the surface of the nanoparticles was modified with 2 bromoisovaleric acid (Br-iVA), cetyl alcohol (CtA), and 3-aminopropyltriethoxysilane (APTES). PQDs modified with Br-iVA exhibited the highest stability in polar solvents and water, maintaining for up to 90 days.

KEYWORDS perovskite quantum dots, ligand-assisted re-precipitation, halide-exchange method, modification PQDs.

ACKNOWLEDGEMENTS This work was supported by the Russian Science Foundation under grant No. 24-23-00432.

FOR CITATION Novikova S.A., Gribova E.D., Kasimtseva K.S., Sidorov E.A., Fadeikina I.N., Nechaev A.N. A surface modification strategy for synthesizing highly water-stable $CsPbBr_3$ perovskite quantum dots. *Nanosystems: Phys. Chem. Math.*, 2025, **16** (4), 521–527.

1. Introduction

Perovskite quantum dots (PQDs) have garnered significant attention of researchers due to its exceptional properties. These unique characteristics position PQDs as viable alternatives to conventional organic luminophores. PQDs have found broad applications across diverse scientific and technological field, demonstrating promising potential for biomedical applications, particularly as biomolecular labels [1]. A common approach involves conjugating PQDs with biomolecules. Protein-conjugated PQDs have been applied in various bioanalytical techniques, including immunoassays, drug delivery tracking, and the visualization of affected tissues [2, 3]. The crucial properties of PQDs essential for medical diagnostics include: high fluorescence intensity; narrow photoluminescence peaks with full widths at half maximum (FWHM) typically ranging from 10 to 35 nm, enabling the simultaneous use of multiple fluorescent probes; tunable emission across the visible spectrum through controlled stoichiometry; and high resistance to defects coupled with a high quantum yield of photoluminescence (>90%) [4].

Halide perovskites with the composition $CsPbX_3$ (X = Br, Cl, I) have exhibited enhanced stability compared to other types of PQDs. Notably, their emission spectra can be tailored across the entire visible and near-infrared (NIR) range by adjusting the halogen ratio within the QDs [5, 6]. This NIR emission capability is particularly advantageous for medical applications, as biological tissues possess a transparency window within this spectral range, minimizing the absorption of electromagnetic radiation between 650 and 1350 nm. Despite these promising attributes, halide cesium-lead PQDs of the $CsPbX_3$ composition face several limitations for *in vivo* medical diagnostics, primarily due to their toxicity arising from the presence of heavy metals, particularly lead [7–9]. The studies [10–12] have demonstrated that chemical modification of PQDs and the application of an inert shell can mitigate these toxic effects. Additionally, the application of PQDs may be limited to *in vitro* research and diagnostics, where the toxicity issue is less acute and does not significantly restrict the types of QDs used.

The conjugation of PQDs with biomolecules is a required for their application in medical diagnostics. This process must be conducted without significantly compromising the properties and functionality of the PQDs [13]. Despite the common use of water-soluble PQDs for conjugation, their susceptibility to rapid degradation and decomposition in polar media remains a significant challenge. Ensuring the long-term stability and high fluorescence of halide PQDs is essential for their widespread application.

To overcome these challenges, various strategies have been employed, including surface modification of PQDs with a shell [1, 14], replacement of hydrophobic surface ligands with hydrophilic ones [14, 15], and doping with atoms of different elements [16–18]. Silicon and titanium oxides, as well as a variety of synthetic polymers, are commonly used as shells of QDs [19, 20], while short-chain amines and carboxylic acids serve as hydrophilic ligands [21, 22]. These approaches have significantly enhanced the stability of PQDs for both air and polar solvent environments.

It is crucial to study the influence of synthesis conditions and surface modification on the spectral characteristics and properties of PQDs for their application in bioanalysis. Two widely used methods for producing PQDs are the hot injection method and the ligand-assisted reprecipitation (LARP) method. PQDs are typically synthesized in nonpolar organic solvents, and ensuring their stability in polar media remains a significant challenge. The objective of this work is to synthesize halide cesium-lead PQDs, characterize their physicochemical properties and stability, and assess the impact of modifications in polar environments.

2. Materials and methods

2.1. Materials

Cesium bromide (CsBr, Alfa Aesar, 99.999 %); lead bromide ($PbBr_2$, ChimKraft, pure for analysis); dimethylformamide (DMF, Komponent Reaktiv, 99.9 %); oleic acid ($C_{17}H_{33}COOH$, Sigma Aldrich, 90 %); 2-bromoisovaleric acid (Br–iVA, $C_5H_9O_2Br$, Alfa Aesar, 99 %); octadecylamine (OAm) ($C_{18}H_{39}N$, Acros Organics, 90 %); cetyl alcohol (CtA, $C_{16}H_{34}O$, Leap Chem CO., $\geq$ 99 %); 3-aminopropyltriethoxysilane (APTES) (Wacker, $>$ 99.0 %); toluene (Panreac Applichem, ACS, dry); benzene (Panreac Applichem, 99.5 %); diethyl ether (Panreac Applichem, 99.7 %); chloroform (Panreac Applichem, reagent USP, Ph. Eur.); acetonitrile (Cryochrom, grade 0); hexane (Sigma Aldrich, $\geq$ 99 %); 1-octadecene (Acros organics, 90 %); ethyl alcohol medical (Ferein, 95 %); deionized water.

2.2. Preparation and purification $CsPbBr_3$ QDs

Initially, 35 mM CsBr and 35 mM $PbBr_2$ were placed in a flat-bottom flask. Then the required amount of octadecylamine (OAm) and oleic acid (OA) was added, and the mixture was stirred without heating. Following this, 0.08 mol of DMF was added to the flask, raising the temperature of the reaction mixture to 120–130°C. The volume ratio of DMF:OA:OAm was maintained at 20:2:1. The resulting reaction mass was quickly transferred into an antisolvent with vigorous stirring. Toluene, benzene, diethyl ether and chloroform were used as antisolvents in this study.

Finally, the obtained PQDs were isolated by centrifugation at 12,000 g for 5 min with the addition of acetonitrile. The obtained PQDs were additionally washed once with an antisolvent and dried in air, preparation PQDs in powder forms.

2.3. Preparation 2-bromoisovaleric acid-$CsPbBr_3$ QDs

The synthesis was conducted following to the protocol described in section 2.2. The salts were dissolved in DMF in the presence of surfactants: Br-iVA and OAm. The volume ratio of DMF:Br-iVA:OAm was maintained at 20:2:1. After purification, the precipitated PQDs were dried in air and redispersed in 1 ml of deionized water by a vortex.

2.4. Preparation Cetyl alcohol-$CsPbBr_3$ QDs

To the dry $CsPbBr_3$ PQDs obtained following the protocol described in 2.2, 0.08 mol of a cetyl alcohol (CtA) solution in toluene was added with stirring for 1,5 h at room temperature. After that, the resulting coated PQDs solution was purified by centrifugation at 12,000 g for 5 min with acetonitrile. Subsequently, the supernatant was separated, the obtained PQDs were washed once with an antisolvent and dried in air. The dried CtA-$CsPbBr_3$ PQDs in powder forms were redissolved in the selected antisolvent, stirring vigorously with a vortex.

2.5. Preparation of 3-Aminopropyltriethoxysilane-Cetyl alcohol-$CsPbBr_3$ QDs

To the CtA-$CsPbBr_3$ PQDs in toluene, an alcoholic solution of APTES was added dropwise with stirring for 24 h at room temperature. The volume ratio of APTES to CtA-$CsPbBr_3$ was maintained at 1:10. After that, the resulting coated PQDs solution was purified by centrifugation at 12,000 g for 5 min with acetonitrile. Subsequently, the supernatant was separated, and the PQDs were washed once with toluene and dried in air. Finally, the dried APTES-CtA-$CsPbBr_3$ PQDs in powder forms were redispersed in the selected antisolvent, stirring vigorously with a vortex.

2.6. Characterization of PQDs

Fluorescence and absorption spectra were recorded by fluorescence spectrometer (Solar CM2203, Belarus). Infrared absorption spectra were obtained with a FTIR spectrometer (Nicolet iS10, USA. Particle size distribution was analyzed by dynamic light scattering (DLS, Malvern Zetasizer Nano ZS, UK). The morphology was characterized by scanning electron microscope (SEM, HITACHI SU 8020, Japanese), centrifuge (Thermo Scientific Sorvall ST 16R).

3. Results and discussion

3.1. Characte rization of hydrophobic PQDs $CsPbBr_3$

In this study, $CsPbBr_3$ PQDs were synthesized using the ligand-assisted re-precipitation (LARP) method, a simpler and more accessible approach compared to the hot injection method, which requires high temperatures and an inert atmosphere.

Several studies [23, 24] have reported the preparation of colloidal PQDs solutions using the LARP method. In this study, we introduced modifications to the synthesis by adjusting the composition and ratio of surfactants. It is well-established that key factors influencing the properties of synthesized quantum dots include solvent type, reaction temperature and time. The synthesis in this study was conducted under heated conditions, with the maximum temperature determined by the solvent's boiling point. Given DMF's boiling point of 153°C, a synthesis temperature of 130°C was selected. This modification resulted in a significant increase in the formation rate of PQDs compared to synthesis at room temperature. The hydrodynamic size of the $CsPbBr_3$ PQDs in toluene was measured to be 23 ± 3 nm by DLS.

To study the effect of the antisolvent nature on PQDs synthesis, a comparative analysis was performed using several nonpolar solvents, including toluene benzene, diethyl ether and chloroform (Fig. 1a,b). $CsPbBr_3$ PQDs exhibited the highest solubility in benzene and toluene, which could be attributed to the low dipole moments of these solvents (dipole moments of benzene and toluene are 0 and 0.40 D, respectively) and the presence of delocalized π-bonds in their molecules. In contrast, hexane, despite having a dipole moment of 0.08 D, does not contain delocalized π-bonds.

The absorption spectra of $CsPbBr_3$ PQDs synthesized in the selected antisolvents exhibited a well-defined excitonic band (Fig. 1a), with the maximum ranging from 420 to 460 nm for benzene, chloroform, and diethyl ether.

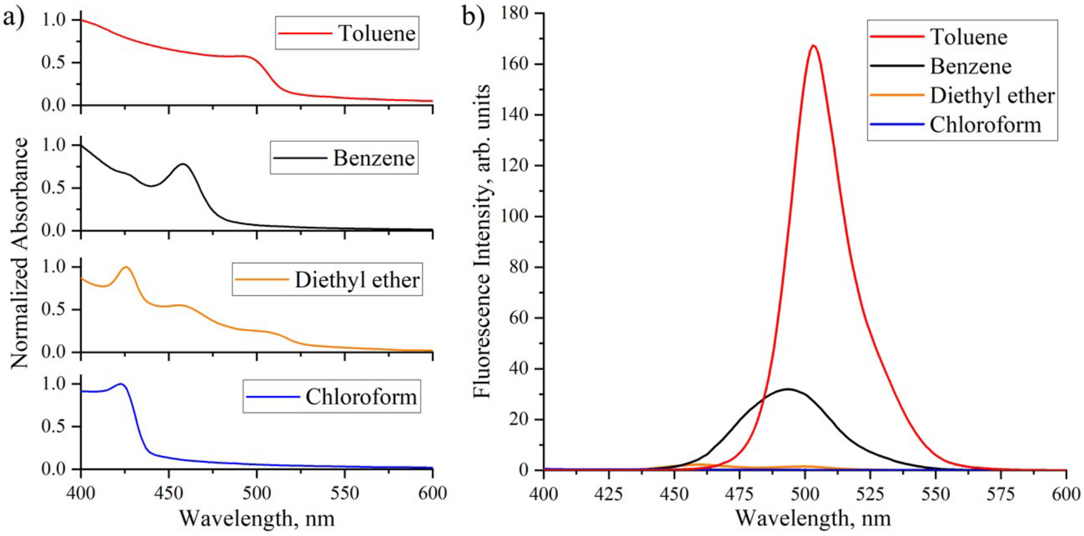

FIG. 1. Optical properties of $CsPbBr_3$ PQDs synthesized in toluene, benzene, diethyl ether and chloroform: a) normalized absorption spectra; b) fluorescence spectra

However, in toluene, the excitonic band is red-shifted, which can be attributed to the quantum confinement effect resulting from changes in the size of the nanoparticles. Notably, a narrow and symmetric fluorescence peak is observed only for PQDs synthesized in benzene and toluene (Fig. 1c). PQDs obtained with other solvents exhibit a relatively broad and asymmetric fluorescence peak with a significant decrease in intensity. A potential explanation for this lies in the ability of non-polar solvents to strip ligands from the surface, an effect not observed with benzene and toluene, which fully retains the ligand layer [26]. In contrast to diethyl ether, hexane, chloroform, benzene and toluene have delocalized π-bonds that create a π-electron system that interacts with PQDs. Cesium (Cs^+), lead (Pb^{2+}) ions on the surface of PQDs can interact with the π-electron system of benzene and toluene, there by stabilizing them on the surface and reducing surface defects [27]. This makes these solvents unsuitable for PQD synthesis. Therefore, benzene and toluene were selected as antisolvents for further synthesis and characterization of PQDs.

3.2. Characterization of water-soluble PQDs $CsPbBr_3$

PQDs hold great promise for bioanalytical applications, but their stability in polar media remains a significant challenge. To address this limitation, we modified the surface of PQDs with 2-bromoisovaleric acid (Br-iVA). The carboxylic groups of Br-iVA and the amino groups of OAm orient towards the PQD surface, forming a protective shell of alkyl groups around the $CsPbBr_3$ core and preventing water molecules from penetrating and quenching fluorescence. Following dispersion in water, the resulting Br-iVA-$CsPbBr_3$ PQDs exhibit sustained high fluorescence intensity for several days. Additionally, the introduction of the bromine atom in BriVA enhances the hydrophilicity of the PQDs. Fig. 2 illustrates a proposed scheme for the synthesis of these water-soluble PQDs, which involves the replacement of the long-chain OA ligand with the shorter Br-iVA.

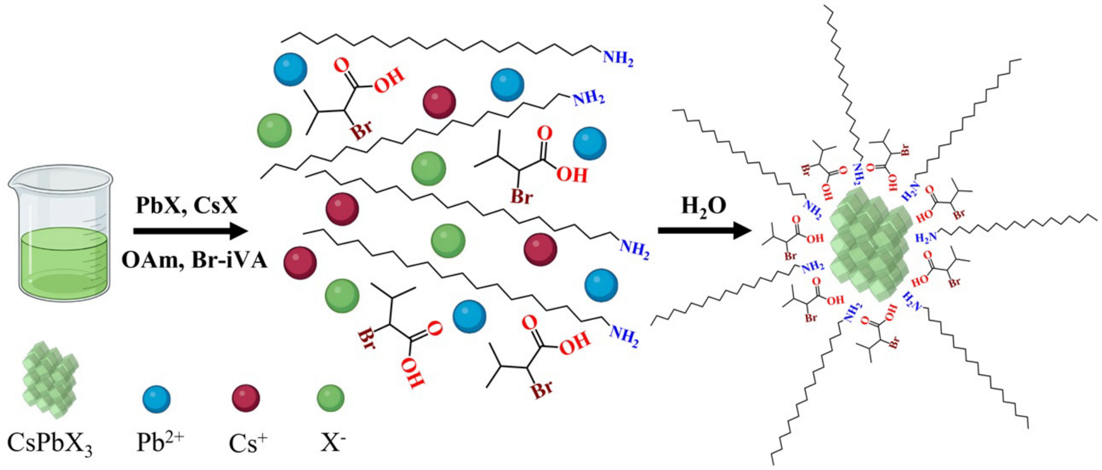

FIG. 2. Schematic representation of water-soluble PQDs synthesis by ligand exchange

The absorption spectra of Br-iVA-CsPbBr$_3$ PQDs exhibited an intense excitonic band, confirming the formation of quantum dots. The narrow and symmetric fluorescence peak indicated a high degree of homogeneity (Fig. 3a).

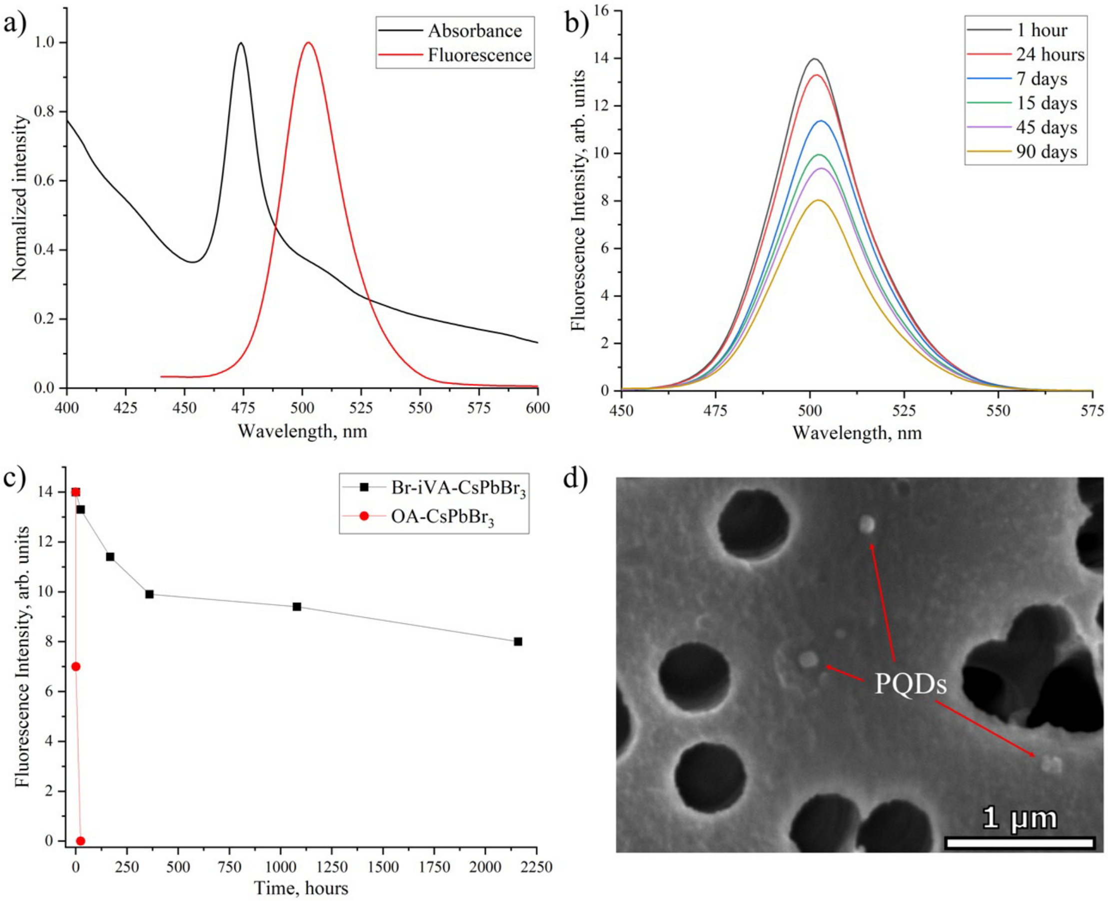

FIG. 3. a) Absorption and fluorescence spectra of Br-iVA-CsPbBr$_3$ PQDs in water; b) Fluorescence spectra of Br iVA-CsPbBr$_3$ PQDs aqueous solution over 90 days; c) Comparison of luminescence intensity between OA-CsPbBr$_3$ PQDs and Br-iVA-CsPbBr$_3$ PQDs; d) SEM image of Br-iVA-CsPbBr$_3$ PQDs deposited on a polyethyleneimine-modified track membrane

The synthesized PQDs maintained high fluorescence intensity in aqueous solution for several days, with the emission peak remaining at 503 nm (Fig. 3b). The PQDs exhibited exceptional long-term stability in water, lasting up to 90 days. Fig. 3c demonstrates a minimal decline in fluorescence intensity, with a reduction of only 4 % from the initial value over 7 days. Subsequently, the fluorescence intensity remained relatively stable for the remaining 83 days. In contrast, PQDs obtained using OA exhibited a rapid and substantial decrease in fluorescence intensity, dropping to 1% of the initial value within 30 minutes of dispersion in water. Fig. 3d presents an SEM image of the synthesized Br-iVA-CsPbBr$_3$ PQDs deposited on a polyethyleneimine-modified track membrane.

Fig. 4a show the TEM images and corresponding particle size distribution of cubic Br-iVA-CsPbBr$_3$ PQDs. The highly structured PQDs are of a particle size of 17.8 ± 2 nm. The image in Fig. 4b highlights that Br-iVA-CsPbBr$_3$ PQDs possess a well-defined crystalline structure with a cubic lattice parameter of 0.56 nm. The image in Fig. 4c indicates that the PQDs have a high crystallinity.

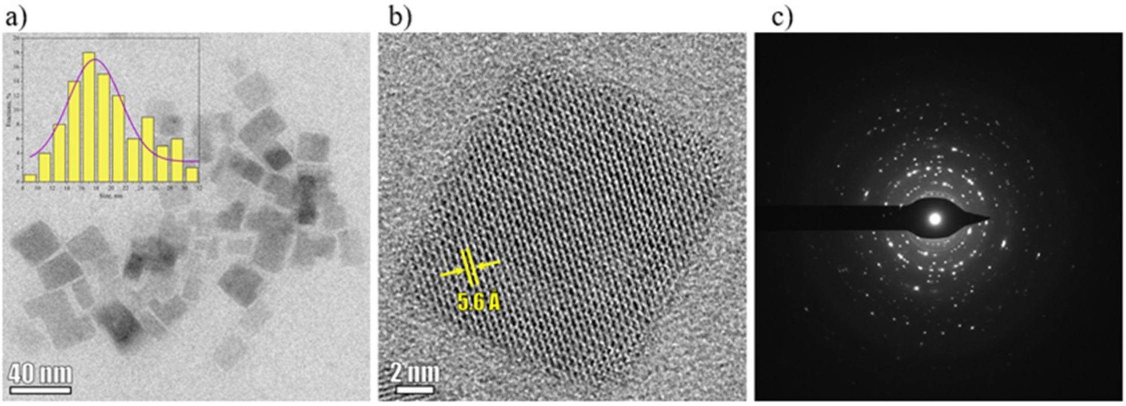

FIG. 4. a) TEM images of Br-iVA-CsPbBr$_3$ PQDs; b) High-resolution imaging of single PQDs; c) TEM micro diffraction pattern

Despite the water solubility and stability of Br-iVA-CsPbBr$_3$ PQDs in polar media, surface modification remains crucial for bioconjugation. To address this, we introduce a novel approach involving the addition of cetyl alcohol (CtA) to pre-synthesized PQDs. CtA coats the PQD surface through dispersion interactions with OA and OAm, while orienting the hydroxyl groups outward (Fig. 5). The resulting CtA-CsPbBr$_3$ PQDs exhibit enhanced stability in aqueous media. However, their stability, lasting approximately 5 days, falls between that of OA-CsPbBr$_3$ and BriVA-CsPbBr$_3$ PQDs.

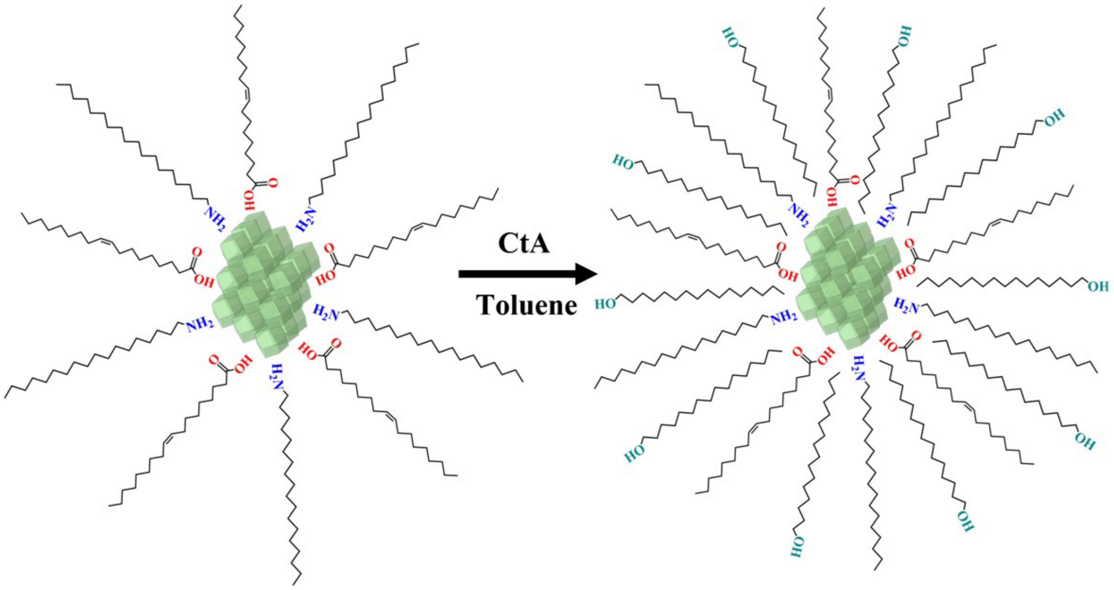

FIG. 5. Schematic representation of CsPbBr$_3$ PQD modification with CtA

To enhance stability and enable protein conjugation, we modified CtA-capped PQDs with APTES. APTES undergoes hydrolysis, forming silanol groups that condense to form a protective siloxane shell around the CtA-CsPbBr$_3$ PQDs. This shell protects the PQD core from degradation in polar media. The resulting APTES-CtA-CsPbBr$_3$ PQDs were characterized by Fourier transform infrared spectroscopy (FTIR) (Fig. 6a). FTIR analysis revealed several characteristic peaks. A broad band ranged between 3500–3200 cm^{-1} was assigned to the stretching vibrations of the hydroxyl (–OH) group. The asymmetric stretching vibrations of the (–C–H) bond were observed at 2940–2915 cm^{-1}, while the bending vibrations of the same bond were located at 1480–1440 cm^{-1}. A medium-intensity peak at 1650–1580 cm^{-1} was attributed to the bending vibrations of the –NH group. The presence of a band at 515–680 cm^{-1} is indicative of the (C–Br) bond, and the band at 1100–1000 cm^{-1} is consistent with the stretching vibrations of the (Si–O–Si) bond. These findings provide strong evidence for the formation of –Si–O–Si– bonds on the PQDs surface.

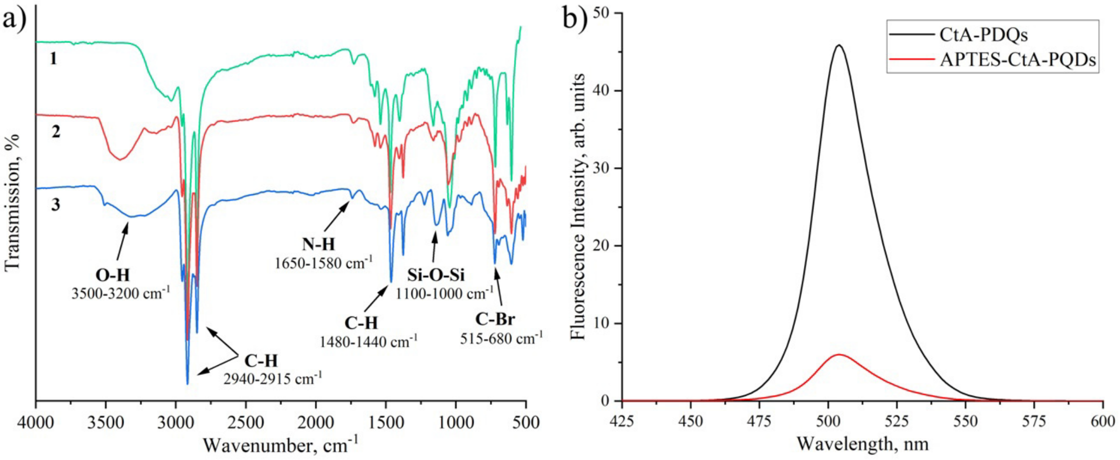

FIG. 6. a) FTIR spectra of $CsPbBr_3$ PQDs (1), CtA-$CsPbBr_3$ PQDs (2), and CtA-APTES-$CsPbBr_3$ PQDs (3); b) Fluorescence spectra of CtA-$CsPbBr_3$ and CtA-APTES-$CsPbBr_3$ PQDs

The size of the CtA-$CsPbBr_3$ nanocrystals in water was 93 ± 5 nm by DLS, while the size of the APTES-modified nanocrystals in water increased slightly to 95 ± 11 nm.

Notably, the fluorescence intensity of the synthesized PQDs decreased significantly upon the addition of an ethanolic APTES solution (Fig. 6b). This occurrence can be attributed to the excess of APTES, which forms an uncontrollable rigid silica matrix [25], leading to particle aggregation and subsequent fluorescence quenching. PQDs with the composition APTES-CtA-$CsPbBr_3$ exhibited stability only in ethanol and were unstable in aqueous media, likely due to the ongoing hydrolysis of APTES, resulting in the disruption of the PQD structure.

Thus, this research successfully achieved its primary objective of synthesizing highly water-stable $CsPbBr_3$ PQDs for bioanalytical applications.

4. Conclusion

In summary, we successfully synthesized $CsPbBr_3$ PQDs via a LARP method. Toluene and benzene were identified as the optimal antisolvents for this process. Two approaches were studied to enhance the stability of PQDs in aqueous media. The first approach involved ligand exchange, replacing long-chain OA with short-chain Br-iVA, which significantly enhanced the stability of PQDs in polar solvents (up to 90 days). The second approach focused on modifying the surface of PQDs with CtA and APTES, enabling potential applications in bioanalysis. While the stability of the surface-modified PQDs in water was increased compared to hydrophobic counterparts, it remained insufficient for biomedical applications. Comprehensive characterization of the synthesized PQDs using various techniques (spectroscopy, SEM, DLS) confirmed the efficacy of both approaches in enhancing stability.

Consequently, increasing the stability of PQDs in polar media remains a significant challenge due to their susceptibility to degradation under various conditions. Therefore, the synthesis, characterization, and surface modification of PQDs continue to be active areas of research.

References

[1] Talianov P.M., Peltek O.O., Masharin M., Khubezhov S., Baranov M.A., Drabavicius A., Timin A.S., Zelenkov L.E., Pushkarev A. P., Makarov S.V., Zyuzin M.V. Halide perovskite nanocrystals with enhanced water stability for upconversion imaging in a living cell. *The Journal of Physical Chemistry Letters*, 2021, **12**(37), P. 8991–8998.

[2] Zhao Y., Zhang Q., Meng Q., Wu F., Zhang L., Tang Y., Guan Y. An L. Quantum dots-based lateral flow immunoassay combined with image analysis for semiquantitative detection of IgE antibody to mite. *International Journal of Nanomedicine*, 2017, P. 4805–4812.

[3] Matea C.T., Mocan T., Tabaran F., Pop T., Mosteanu O., Puia C., Iancu C., Mocan L. Quantum dots in imaging, drug delivery and sensor applications. *International Journal of Nanomedicine*, 2017, P. 5421–5431.

[4] Wang Y.K., Yuan F., Dong Y., Li J.Y., Johnston A., Chen B., Saidaminov M.I., Zhou C., Zheng X., Hou Y., Bertens K., Ebe H., Ma D., Deng Z., Yuan S., Chen R., Sagar L. K., Liu J., Fan J., Li P., Li X., Gao Y., Fung M., Lu Z., Bakr O.M., Liao L., Sargent E.H. All-inorganic quantum-dot LEDs based on a phase-stabilized α-$CsPbI_3$ perovskite. *Angewandte Chemie International Edition*, 2021, **60**(29), P. 16164–16170.

[5] Koryakina I., Kuznetsova D.S., Zuev D.A., Milichko V.A., Timin A.S., Zyuzin M.V. Optically responsive delivery platforms: From the design considerations to biomedical applications. *Nanophotonics*, 2020, **9**(1), P. 39–74.

[6] Lian H., Li Y., Saravanakumar S., Jiang H., Li Z., Wang J., Xu L., Zhao W., Han G. Metal halide perovskite quantum dots for amphiprotic bio-imaging. *Coordination Chemistry Reviews*, 2022, **452**, P. 214313.

[7] Seo H.K., Kim H., Lee J., Park M.H., Jeong S.H., Kim Y.H., Kwon S., Han T., Yoo S., Lee T.W. Efficient flexible organic/inorganic hybrid perovskite light-emitting diodes based on graphene anode. *Advanced Materials*, 2017, **29**(12), P. 1605587.

[8] Wang F., Wang H., Ali A., Zhang Y., Cui X., Liu Y. In-situ one-step electrospray fabrication of polyvinylidene fluoride encapsulated CsPbBr$_3$ spheres with high stability and cell imaging application. *Inorganic Chemistry Communications*, 2019, **106**, P. 99–103.

[9] Jiang G., Erdem O., Hübner R., Georgi M., Wei W., Fan X., Wang J., Demir H.V., Gaponik N. Mechanosynthesis of polymer-stabilized lead bromide perovskites: Insight into the formation and phase conversion of nanoparticles. *Nano Research*, 2021, **14**, P. 1078–1086.

[10] De Albuquerque C.D.L., Schultz Z.D. Super-resolution surface-enhanced Raman scattering imaging of single particles in cells. *Analytical Chemistry*, 2020, **92**(13), P. 9389–9398.

[11] Min Q., Lei J., Guo X., Wang T., Yang Q., Zhou D., Yu X., Yu S. F., Qiu J., Zhan Q., Xu X. Atomic-level passivation of individual upconversion nanocrystal for single particle microscopic imaging. *Advanced Functional Materials*, 2020, **30**(6), P. 1906137.

[12] Oh H., Park Y., Song H. Tracking underpotential deposition of copper on individual silver nanocubes by real-time single-particle plasmon scattering imaging. *The Journal of Physical Chemistry C*, 2020, **124**(37), P. 20398–20409.

[13] Zheng J., Chen J., Sun R., Zhang W., Huang Y., Shao J., Chi Y. A fluorescent immunochromatographic strip based on CsPbBr$_3$/CsPb$_2$Br$_5$@ SiO$_2$ facile encapsulation in pure water for the detection of human chorionic gonadotropin (HCG) antigen. *Sensors and Actuators B: Chemical*, 2024, **410**, P. 135608.

[14] Hsieh Y.T., Lin Y.F., Liu W.R. Enhancing the water resistance and stability of CsPbBr$_3$ perovskite quantum dots for light-emitting-diode applications through encapsulation in waterproof polymethylsilsesquioxane aerogels. *ACS Applied Materials & Interfaces*, 2020, **12**(52), P. 58049–58059.

[15] Loiudice A., Saris S., Oveisi E., Alexander D.T., Buonsanti R. CsPbBr$_3$ QD/AlOx inorganic nanocomposites with exceptional stability in water, light, and heat. *Angewandte Chemie International Edition*, 2017, **56**(36), P. 10696–10701.

[16] Bi C., Wang S., Li Q., Kershaw S. V., Tian J., Rogach A.L. Thermally stable copper (II)-doped cesium lead halide perovskite quantum dots with strong blue emission. *The Journal of Physical Chemistry Letters*, 2019, **10**(5), P. 943–952.

[17] Li S., Shi Z., Zhang F., Wang L., Ma Z., Yang D., Yao Z., Wu D., Xu T., Y. Tian, Zhang Y., Shan C., Li X. J. Sodium doping-enhanced emission efficiency and stability of CsPbBr$_3$ nanocrystals for white light-emitting devices. *Chemistry of Materials*, 2019, **31**(11), P. 3917–3928.

[18] Yao J.S., Ge J., Han B.N., Wang K.H., Yao H.B., Yu H.L., Li J.H., Zhu B.S., Song J., Chen C., Zhang Q., Zeng H., Luo Y., Yu S.H. Ce^{3+}-doping to modulate photoluminescence kinetics for efficient CsPbBr$_3$ nanocrystals based light-emitting diodes. *Journal of the American Chemical Society*, 2018, **140**(10), P. 3626–3634.

[19] Reiss P., Protiere M., Li L. Core/shell semiconductor nanocrystals. *Small*, 2009, **5**(2), P. 154–168.

[20] Ghosh Chaudhuri R., Paria S. Core/shell nanoparticles: classes, properties, synthesis mechanisms, characterization, and applications. Chemical Reviews, 2012, **112**(4), P. 2373–2433.

[21] Liu Z., Zhang Y., Fan Y., Chen Z., Tang Z., Zhao J., Lv Y., Lin J., Guo X., Zhang J., Liu X. Toward highly luminescent and stabilized silica-coated perovskite quantum dots through simply mixing and stirring under room temperature in air. *ACS Applied Materials & Interfaces*, 2018, **10**(15), P. 13053–13061.

[22] Li Q., Xu K., Fan S., Zhang H., Wei X., Xu C., Luan X., Wang Z. X., Peng H., Shi L. Two Birds with One Stone: Aqueous Phase Synthesis of All-Inorganic Halide Perovskite CsPbClxBr3-x Nanocrystals Using Cstfa as Cesium Source and Surface Ligand. *Available at SSRN* 4653908.

[23] Li, X., Wu, Y., Zhang, S., Cai, B., Gu, Y., Song, J., & Zeng, H. CsPbX3 quantum dots for lighting and displays: room-temperature synthesis, photoluminescence superiorities, underlying origins and white light-emitting diodes. *Advanced Functional Materials*, 2016, **26**(15), P. 2435–2445.

[24] Zhang J., Fan L., Li J., Liu X., Wang R., Wang L., & Tu G. Growth mechanism of CsPbBr$_3$ perovskite nanocrystals by a co-precipitation method in a CSTR system. *Nano Research*, 2019, **12**, P. 121–127.

[25] Woźnica M., Sobiech M., Luliński P. A fusion of molecular imprinting technology and siloxane chemistry: A way to advanced hybrid nanomaterials. *Nanomaterials*, 2023, **13**(2), P. 248.

[26] Han S. et al. Stabilized perovskite quantum dot solids via nonpolar solvent dispersible covalent ligands. *Advanced Science*, 2023, **10**(23), P. 2301793.

[27] Lao Y., Yang S., Yu W., Guo H., Zou Y., Chen Z., & Xiao L. Multifunctional π-Conjugated Additives for Halide Perovskite. *Advanced Science*, 2022, **9**(17), P. 2105307.

Submitted 10 October 2024; revised 30 March 2025, 23 June 2025; accepted 1 August 2025

Information about the authors:

Sagila A. Novikova – Dubna State University, Dubna, Moscow oblast, 141980, Russia; sagila@uni-dubna.ru

Elena D. Gribova – Dubna State University, Dubna, Moscow oblast, 141980, Russia; elena_g67@mail.ru

Ksenia S. Kasimtseva – Dubna State University, Dubna, Moscow oblast, 141980, Russia; kasimtseva20@yandex.ru

Evgeniy A. Sidorov – Dubna State University, Dubna, Moscow oblast, 141980, Russia; zhenya.sidorov1@gmail.com

I. N. Fadeikina – Joint Institute for Nuclear Research, Dubna, Moscow oblast, 141980 Russia

A. N. Nechaev – Joint Institute for Nuclear Research, Dubna, Moscow oblast, 141980 Russia

Conflict of interest: the authors declare no conflict of interest.